

Planning for the 2023 and 2024 Solar Eclipses at VHF, UHF and Ku-band

Christian Monstein and Whitham D. Reeve

1. Introduction

The annular solar eclipse (ASE) and total solar eclipse (TSE) forecasted to occur on 14 October 2023 and 8 April 2024, respectively, (figure 1) provide two wonderful opportunities for observing related radio phenomena over a wide frequency range. Observations of at least partial eclipses are possible over much of North and South America (2023 eclipse) and much of North America and even Greenland (2024 eclipse). Almost all states in the USA will be able to view at least a part of the two eclipses, but observations are not limited to just the USA.

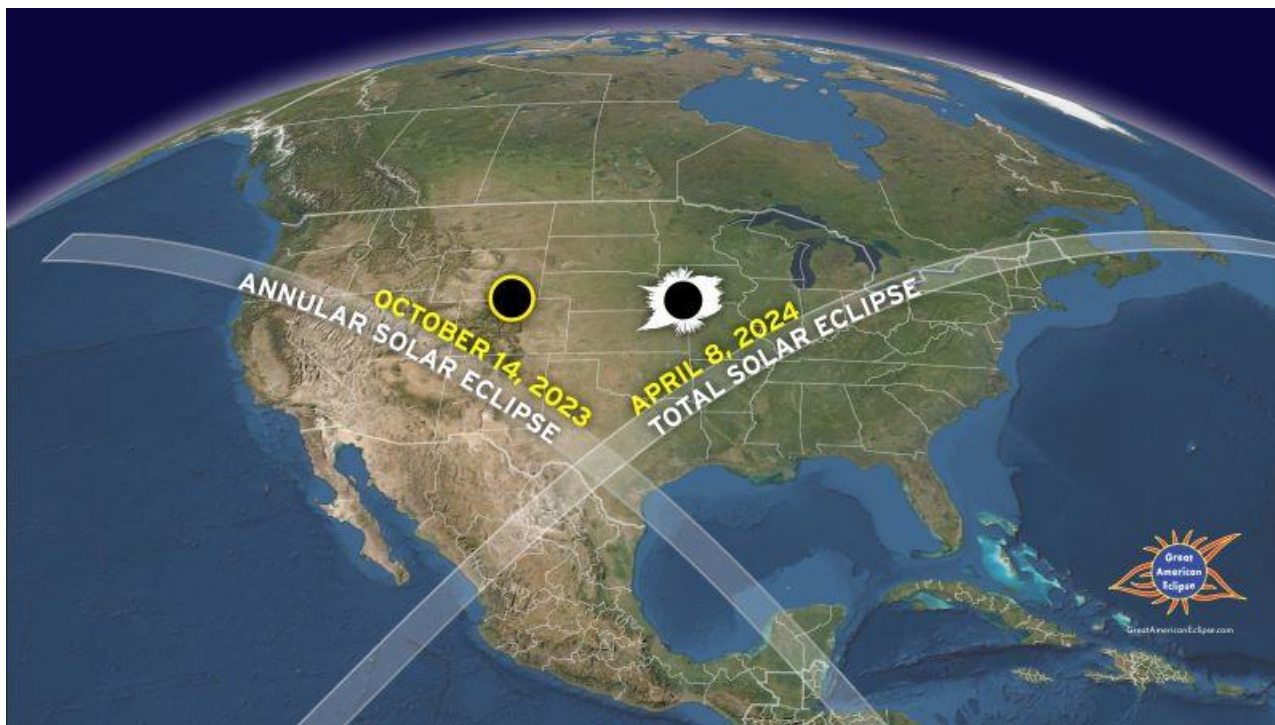


Figure 1 ~ View of the October 2023 and April 2024 eclipse paths over North America. Image source: <https://earthsky.org/sun/annular-solar-eclipse-october-14-2023/>

The current paper primarily concerns direct solar radio observations during the eclipses in the very high frequency (VHF, 30 to 300 MHz), ultrahigh frequency (UHF, 300 to 3 000 MHz) and super high frequency (SHF, 3 000 to 30 000 MHz) bands. We do not cover eclipse effects in the very low frequency (VLF, 3 to 30 kHz) and low frequency (LF, 30 kHz to 300 kHz) but these ranges are worth observing as well.

In particular, we focus on the native frequency range of the Callisto solar radio spectrometer, 45 to 870 MHz, with additional information on using an inexpensive Ku-band satellite dish antenna and associated low noise block converter (LNB) as a down-converter with Callisto to observe in the X-band at about 10 600 MHz. The concepts described in this paper can be applied to other frequency bands with or without the Callisto as an integral part of the radio telescope.

We discuss how to observe changes in solar radio emissions received on Earth's surface as the Sun is occulted by the Moon. At the frequencies of interest, Earth's ionosphere effects are expected to be minor. However, we also discuss how to use Callisto to measure the scintillation index of satellite transmissions in the upper-VHF band during the eclipses.

The eclipses will occur during the rising portion of the current solar cycle 25, so radio observations generally will be of the *active Sun* and its broadband continuum of moderate level radio emissions. A solar radio storm or bursts could occur during the eclipses but such events have low likelihood at X-band.

The current paper provides the forecasted physical characteristics of the two eclipses. We then turn to the higher radio frequencies. Observing a solar eclipse of any kind requires considerable planning, and now is the time to start. Some observers may wish to construct dedicated observing facilities for the eclipses, which will require additional time. Because of the relatively short notice of this article in April 2023, some observers may not have time (6 months) to fully prepare for the October 2023 eclipse, but it nevertheless will provide a good practice session for planning and system setup for the total solar eclipse in April 2024.

Observers should not wait until the last minute. It is very important to pretest the radio spectrometer system long before the event day so that there is plenty of time to become familiar with it and correct any problems. The need for adequate pretesting cannot be overemphasized.

2. Eclipse Characteristics

Solar eclipses of all types (partial, annular, total) are not particularly rare worldwide (for example, see [Solar](#)). Total solar eclipses (TSE), during which the Moon completely occults the Sun, occur somewhere around the world annually but for most of us the opportunity to view a TSE happens only a few times in our lifetime. Annular eclipses also are common but thought to be not as dramatic. During an annular solar eclipse, the Moon is too far from Earth to completely block the Sun but it does occult a good portion of it. During annularity (the maximum phase of an annular eclipse), the Sun appears as an extremely bright ring around the Moon.

On 14 October 2023, the annular solar eclipse will be visible, at least partially, over almost the entire North and South American continents (figure 2). In the USA, the path of annularity starts on the USA west coast in Oregon at 1613 UTC (9:13 am PDT) and ends in Texas at 1703 UTC (12:03 pm CDT). The duration of the optical eclipse will be about 5 min 17 sec at any given location along the annularity path but the duration from start to end of the partial eclipse will be almost 6 h. The Moon will cast a shadow up to 187 km wide as it crosses the United States. Because the eclipse is annular, a portion of the Sun will be visible at all times, and eye protection will be needed during radio telescope alignment.

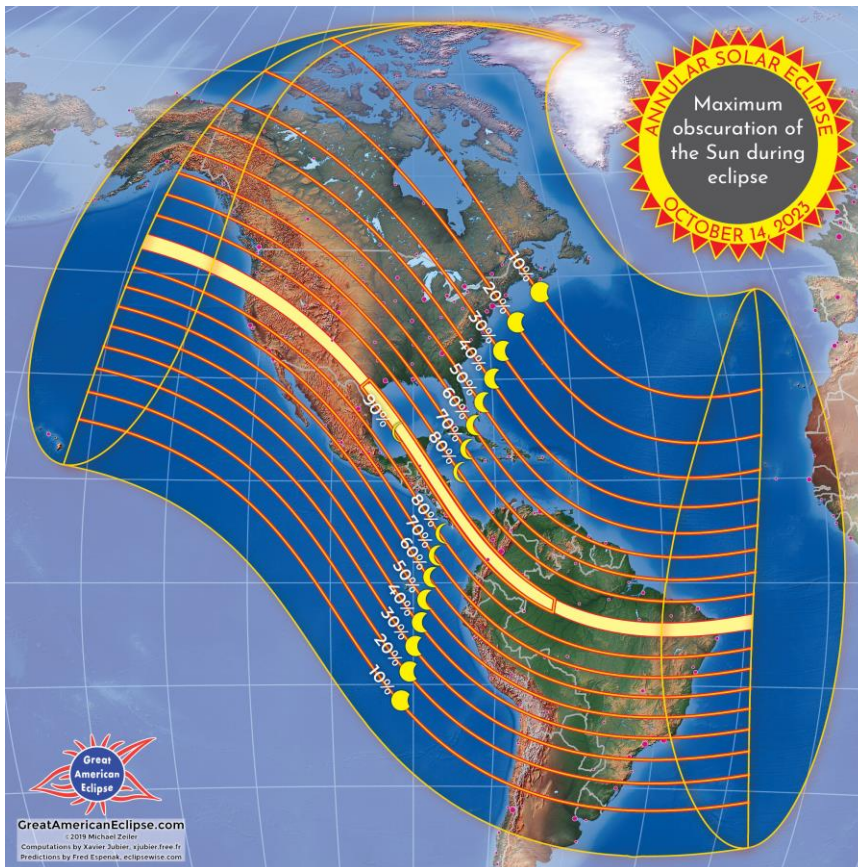


Figure 2 ~ Path of the 2023 annular solar eclipse across Earth's surface. Annularity will be visible within the area outlined by the yellow stripe. The path width is 187.4 km. The northern and southern limits of the eclipse are shown along with the percentage of the eclipse that will be visible at a location. The greatest eclipse location (location of the longest optical eclipse duration) is 11° 21.7' N, 83° 04.3' W, just off the eastern coast of Nicaragua in the Caribbean Sea. The greatest eclipse duration occurs at 17:59:21 UTC and is 5 min 17 s. Image source: <https://earthsky.org/sun/annular-solar-eclipse-october-14-2023/>

On 8 April 2024, a total solar eclipse will be visible in the United States (figure 3). The path of totality – the path where the Moon totally obscures the Sun as viewed from Earth's surface – starts in Texas about 1727 UTC (01:27 pm CDT) and ends in Maine about 1935 UTC (03:35 pm EDT). The duration of total optical eclipse will be about 4 min 27 sec at any given location along the totality path but the duration from start to end of partial eclipse will be almost 3 h. The Moon will cast a shadow up to 197.5 km wide as it crosses the United States.

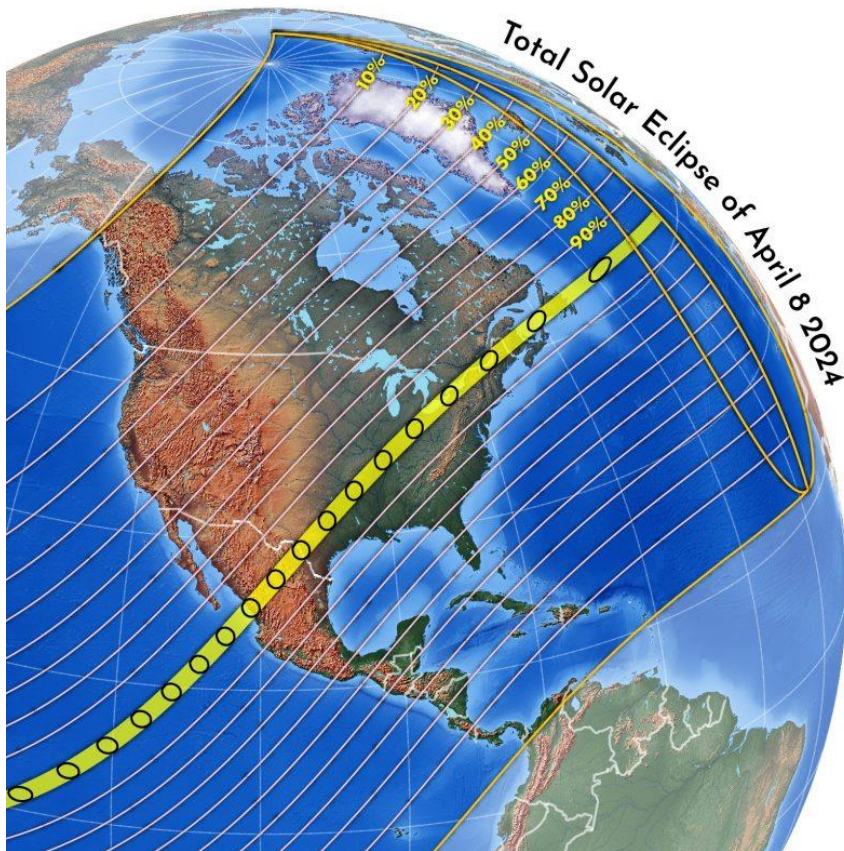


Figure 3 ~ Path of the 2024 solar eclipse across Earth's surface. It will be totally visible within the area outlined by the yellow stripe. The northern and southern limits of the eclipse are shown along with the percentage of the eclipse that will be visible at a location. The greatest eclipse location occurs at 18:17:13 UTC over Durango in northwestern Mexico at 25° 17.5' N, 104° 07.2' W. The longest optical duration is forecasted to be 4 min 27 s. Image source:

<https://earthsky.org/astronomy-essentials/total-solar-eclipse-april8-24/>

2. Radio Emissions from the Quiet Sun

The radio flux from the quiet Sun is a broadband continuum consisting of a steady background component with a constant level lasting months or years and a slowly varying component that changes from day to day with a period of 27 days. These also are called the B- and S-components, respectively. By definition, the quiet Sun produces low level radio emissions.

The background is caused by thermal emissions of the solar atmosphere and is randomly polarized. At frequencies of approximately 30 to 300 MHz the background emissions originate mostly in the solar corona, which is the outer region of the Sun's atmosphere reaching a few solar radii. The corona temperature is about 10^6 kelvin. At higher frequencies up to about 3 GHz the emissions originate partly in the corona and partly in the chromosphere where the temperatures are on the order of 10^4 K. At even higher frequencies, the emissions originate mostly in the chromosphere. Frequencies below 200 MHz are often called *coronal frequencies* and above 10 000 MHz are called *chromospheric frequencies* [Smerd].

The slowly varying component also consists of randomly polarized thermal emissions but these are produced in regions of relatively high electron densities and strong magnetic fields near sunspots and chromospheric plagues (also called plagues). During solar minimum, disturbances from solar flares and other transient phenomena may occasionally and temporarily raise the received radio level above the quiet Sun level.

The spectral flux density of the quiet Sun varies with frequency and rapidly rolls off below about 100 MHz (table 1). The low levels require that the radio telescope has very high sensitivity, which can be attained only by using a low noise amplifier and a high-gain antenna (discussed in sections 6 and 7). The chart indicates the possibility of using a Ku-band dish antenna and associated low noise block converter (LNB) as a down-converter with Callisto (discussed in section 8).

Table 1 ~ Quiet Sun spectral flux densities in solar flux units (sfu) and watts per square meter per Hz at Earth. For reference this chart shows frequencies below and above the Callisto range. Source: [Benz]

Frequency (MHz)	Wavelength (m)	S _{Quiet} (sfu)	S _{Quiet} (W m ⁻² Hz ⁻¹)	Callisto range
30	10	0.17	0.17 · 10 ⁻²²	Up-converter
50	6	0.54	0.54 · 10 ⁻²²	Yes
100	3	2.4	2.4 · 10 ⁻²²	Yes
150	2	5.1	5.1 · 10 ⁻²²	Yes
200	1.5	8.1	8.1 · 10 ⁻²²	Yes
300	1	14.9	14.9 · 10 ⁻²²	Yes
400	0.75	21.7	21.7 · 10 ⁻²²	Yes
600	0.5	32.1	32.1 · 10 ⁻²²	Yes
1000	0.3	41.3	41.3 · 10 ⁻²²	870 MHz
1500	0.2	48.0	48.0 · 10 ⁻²²	Down-converter
3000	0.1	69	69 · 10 ⁻²²	Down-converter
3750	0.08	82	82 · 10 ⁻²²	Down-converter
5000	0.06	107	107 · 10 ⁻²²	Down-converter
10000	0.03	275	275 · 10 ⁻²²	Ku band LNB
15000	0.02	574	574 · 10 ⁻²²	Down-converter

During an eclipse, the received solar radio emissions are reduced as the Moon moves between the Sun and observer. However, unlike the total solar eclipse in visible light, the Sun’s radio emissions are not completely blocked along the path of totality because the radio Sun is much larger than the visible Sun, and a total solar radio eclipse can never occur (figure 4). Similar comments hold for an annular eclipse. The radio Sun at the frequencies of interest is approximately 1.5 to 2 times as wide (east-west) as the visible Sun but roughly the same height (north-south).

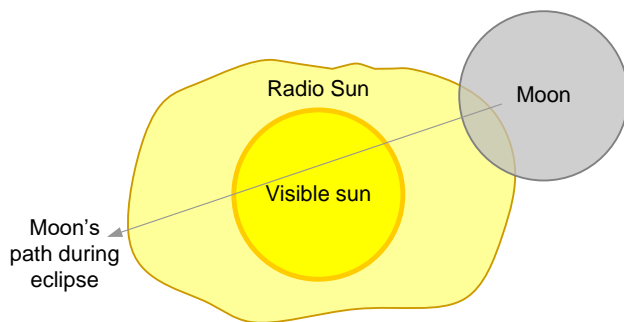


Figure 4 ~ The Moon’s angular size as viewed from Earth is close to the visible Sun’s size, about 0.5°. However, the radio Sun is larger so its radio emissions are not entirely blocked during an eclipse. The radio Sun is asymmetric. The reduction in received flux between the start and end of partial obscuration will span a few hours with some variation at different locations. Image adopted from [Kundu].

The received flux $\psi_{rx}(t)$ during an eclipse is of the form

$$\psi_{rx}(t) = 1 - \psi(t)$$

where $\psi(t)$ is the residual flux as a decimal fraction of the total flux (figure 5).

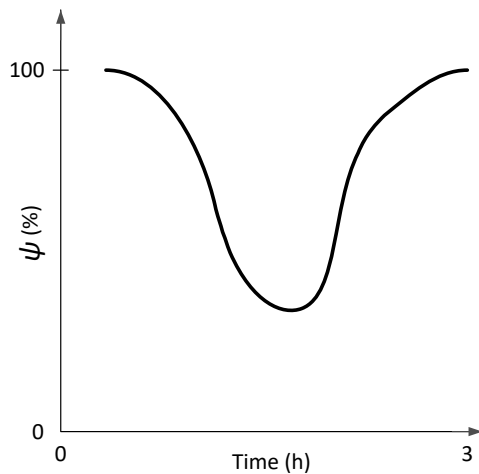


Figure 5 ~ Solar radio flux received on Earth's surface during an eclipse as a percentage of the total flux. The time scale is approximate. Radio observations of the Sun are complicated by the variable component of its emissions and asymmetry of its radio shape. Image adopted from [Kundu].

4. General Considerations

This section provides general considerations and not step-by-step procedures. Each station should formulate detailed observing strategies and procedures and rehearse them well before the eclipse. Although the total eclipse lasts only a few minutes at a given location, the Sun is partially eclipsed for several hours. To obtain comparative data, the Sun should be observed as long as possible before and after the actual eclipse. Two observing modes are described below, Sun tracking and Sun Transit.

Sun tracking mode: The Sun tracking mode requires a 2-axis antenna rotator system that can automatically track the Sun in azimuth and elevation. As a convenient alternative we can use a parallactic mount (also called equatorial mount) where tracking requires only one active drive because the declination of the Sun hardly changes during a few days of observation. The recommended observations span a total of at least seven days – three days before, three days after and the day of the eclipse itself. The pre- and post-eclipse data will be used to establish the quiet Sun emission levels for comparison with the eclipse day. Use the collected data to produce a plot of peak transit intensity over the seven day period as follows (Eclipse day = E):

- | | |
|---------------------|--|
| E-4 day: | Final check of antenna tracking system for proper Sun tracking |
| E-3, E-2, E-1 days: | Observe the Sun to obtain quiet Sun data before eclipse |
| Eclipse day: | Observe as in previous days but expect lower peak intensity during transit |
| E+1, E+2, E+3 days: | Observe the Sun to obtain quiet Sun data after eclipse |

Sun transit (drift) mode: In principle one could observe the eclipse in transit or drift mode where a tracking system is not available. A fixed antenna with 10° beamwidth that is accurately pointed at the midpoint of the total eclipse will view the Sun for approximately 12 min before and 12 min after the midpoint. Therefore, in this case, the Sun will be partially eclipsed when it enters and exits the antenna beam. The observing schedule for

the transit scan is very similar to the tracking mode. Note that the Sun changes position in the sky by a small but significant amount throughout the 7-day observation period:

- E-4 day: Adjust antenna to the sky position of the Sun during eclipse
- E-3, E-2, E-1 days: Observe daily transit to obtain data about quiet Sun level before eclipse
- Eclipse day: Observe as in previous days but expect lower peak intensity during transit
- E+1, E+2, E+3 days: Observe daily transit to obtain data about quiet Sun level after eclipse

The position of the Sun in the sky as seen from the observation point needs to be determined in advance, usually in terms of azimuth and elevation (or altitude). These are easily determined using online calculators such as [{NOAA}](#) or a PC software tool such as the Multiyear Interactive Computer Almanac [\[MICA\]](#). In order to use these tools observers need to know their observatory's geographical location, which can be determined either from a large scale map or Global Navigation Satellite System (GNSS) receiver such as the Global Positioning System (GPS). In addition, one of the authors (Monstein) is able to provide Python scripts for free to perform these calculations.

5. Observed Phenomena

Observations may yield interesting results even for observers who are not along the totality path. The list below provides some ideas for observation. Previous observations of solar eclipses using Callisto are described in [\[Monstein\]](#).

- 1) Width of the radio Sun is almost twice that of the visible Sun
 - 2) Received flux will dip but not disappear during the eclipse
 - 3) Radio brightening at the limb of the optical disk occurs at 200 MHz and above
 - 4) Effects of the eclipse on the scintillation of satellite signals
 - 5) The eclipse can be observed in radio even when the Sun is not visible due to clouds, rain or snowfall.
- Therefore, it is an ideal experiment for outreach during bad weather conditions.

6. Equipment Considerations

This section discusses the requirements for observing the quiet Sun with a radio telescope based on Callisto. Callisto (figure 6) is the instrument portion of the solar radio spectrometer. Callisto has 62.5 kHz frequency resolution throughout its 45 to 870 MHz range, 1 ms integration time, 300 kHz detection bandwidth and 7 dB noise figure. More detailed specifications are at [{Callisto}](#) and information on the e-Callisto network can be found at [eCallisto](#). Callisto by itself is not sensitive enough to observe the quiet Sun, so a low noise amplifier is needed. The entire spectrometer consists of only a few basic components: Callisto, a high-gain antenna, low noise amplifier and associated power coupler (bias-tee), power supply and PC running the Callisto software (figure 7).

For all calculations in this and the next section, the low noise amplifier noise figure is assumed to be 1.1 dB. Actual noise figures for any installation may be substituted with little trouble. For a temporary setup, the low

noise amplifier does not have to be an elaborate weatherproof unit and can be quickly and inexpensively built (figure 8) [ReeveLNA].



Figure 6 ~ Callisto is a channelized sweep-frequency receiver. In most configurations, the channels are swept at a rate of 800 channels/s, but this can be extended to 1000 channels/s when the Callisto is connected to a 1 MHz reference clock source. The Callisto instrument dimensions are 200 x 110 x 82 mm and it weighs 0.9 kg. It is powered by a 12 Vdc power supply and controlled through an EIA-232 interface. Image ©2012 W. Reeve

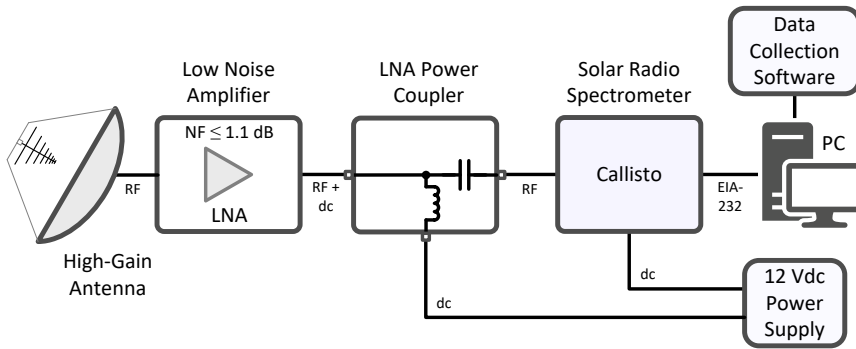


Figure 7 ~ Block diagram showing the basic solar radio spectrometer components. A low noise amplifier and high-gain antenna are critical components required to observe the radio Sun near solar cycle minimum. The LPC contains a bias-tee that allows the LNA to be powered through the coaxial cable to the antenna. Image ©2016 W. Reeve



Figure 8 ~ Inexpensive amplifier package made with a modular low noise amplifier. Dimensions are 110 x 77 x 47 mm and average measured noise figure across the frequency range 45 to 870 MHz is 0.8 dB. This unit requires 12 Vdc at 40 mA, and it can be powered through the coaxial cable using a pair of bias-tees or directly with a separate power cable. It is not weatherproof so it must be covered if there is rain during the eclipse. Image ©2015 W. Reeve

Two factors make detecting the quiet Sun during an eclipse somewhat difficult: First, the received flux levels are very low and the reduction as the Moon moves between the Sun and a terrestrial observer will be small even if the observer is on the path of totality. Thus, the radio telescope must have very high sensitivity, which is obtained by using a high-gain antenna and a low noise amplifier at the antenna. Second, a high-gain antenna may have such a narrow beamwidth that it will be required to accurately track the Sun throughout the eclipse. On the other hand, with a sufficiently sensitive radio telescope using a fixed antenna, a drift scan during the eclipse as previously discussed may yield interesting results.

Many existing Callisto stations use a log periodic dipole array (LPDA) to receive relatively strong solar radio bursts from an active Sun. The gains of typical LPDA antennas range from about 6 to 10 dB and are sufficient to detect strong transient solar radio phenomena above a few hundred solar flux units (sfu). However, the gains are not high enough to allow the Callisto to detect the quiet Sun even with a low noise amplifier at the antenna. Therefore, successful observations during the two eclipses will require both an LNA and an antenna with considerably higher gain. The next section discusses the antenna requirements.

Other Callisto stations use the Long Wavelength Array (LWA) Antenna. The sensitivity of the LWA Antenna and Callisto are approximately the same or better than the LPDA mentioned above. The LWA Antenna has a built-in low noise front end at the antenna hub, but its noise figure is 2.7 dB, somewhat higher than many other types of LNAs that are better than 1 dB.

To illustrate the need for high sensitivity, it is instructive to compare the spectral flux density of the quiet Sun to the sensitivity of a basic Callisto connected to a resistance termination at 290 K and a zero gain antenna (figure 9). For most Callisto stations the quiet Sun flux lies well below the received background when Callisto is connected to such an antenna. Above 600 MHz the quiet radio Sun is close to the noise produced by a room temperature resistance termination.

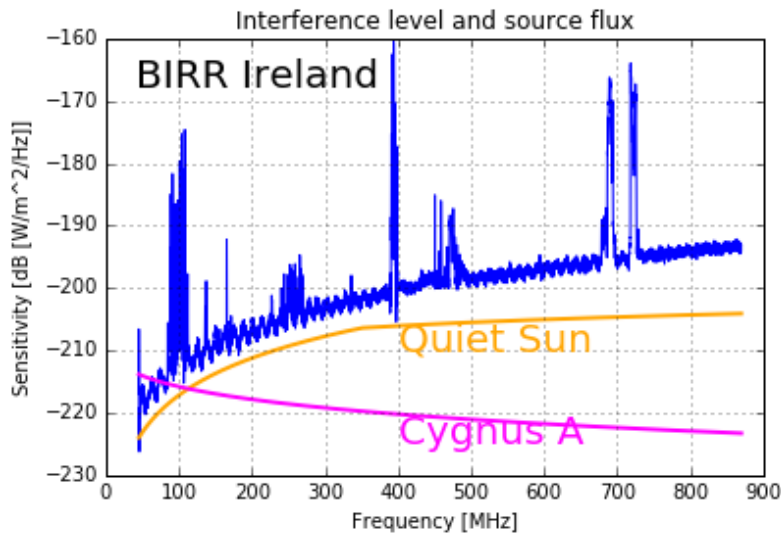


Figure 9 ~ Plot of the expected flux from the quiet radio Sun (orange solid trace) compared to Cygnus A flux (purple solid line) and measured level of rfi (blue solid trace) received by a Callisto and a bicone antenna (essentially a 0 dB gain antenna) at the Birr Observatory in Ireland during a radio frequency interference survey in 2016. This setup did not use an LNA and clearly is unable to detect the quiet Sun. Spikes are transmitters of various types including satellites (particularly around 250 MHz) and broadcast FM and TV stations. Image ©2016 C. Monstein.

7. Antenna Requirements

The antenna requirements for observing the quiet Sun can be determined by considering the system noise as a threshold and then calculating the antenna gain needed to boost the noise produced by the quiet Sun above that threshold. An important ingredient of the system noise calculations is the low noise amplifier noise figure. The calculations below are based on a typical value (1.1 dB) but other noise figures can be substituted.

System noise temperature: The system noise temperature T_{sys} is the sum of the sky noise temperature T_{sky} and the receiver system noise temperature T_{Rx} , or

$$T_{Sys} = T_{Sky} + T_{Rx} \text{ K} \quad (1)$$

The sky noise temperature is a composite of all background sources including the ground at the frequency of interest. For purposes here, it is assumed to be 300 K across the frequency range (the galactic radio background at the low end of the Callisto frequency range can be six times higher). The receiver system noise temperature T_{Rx} is

$$T_{Rx} = T_0 \cdot \left(10^{\frac{NF}{10}} - 1 \right) \quad (2)$$

where $T_0 = 290$ K is the reference temperature and NF is the low noise amplifier noise figure in dB. From eq. (2) for an amplifier noise figure of 1.1 dB (the noise figure is assumed flat across the frequency range and the LNA gain is assumed to be high enough to completely determine the system noise figure)

$$T_{Rx} = T_0 \cdot \left(10^{\frac{NF}{10}} - 1 \right) = 290 \cdot \left(10^{\frac{1.1}{10}} - 1 \right) = 83.6 \text{ K (84 K rounded)}$$

and from eq. (1)

$$T_{Sys} = T_{Sky} + T_{Rx} = 300 + 84 = 384 \text{ K}$$

System noise spectral density: The system noise spectral density NSD_{Sys} is determined from

$$NSD_{Sys} = k \cdot T_{Sys} \quad (3)$$

where k is the Boltzmann constant ($k = 1.38 \cdot 10^{-23} \text{ W Hz}^{-1} \text{ K}^{-1}$). Substituting the system noise temperature into eq. (3) gives the noise spectral density of the system noise floor, or

$$NSD_{Sys} = k \cdot T_{Sys} = 1.38 \cdot 10^{-23} \cdot 384 = 5.3 \cdot 10^{-21} \text{ W Hz}^{-1}$$

With a 1 W reference the noise spectral density in dBW Hz⁻¹ is

$$NSD_{Sys} (\text{dBW / Hz}) = 10 \cdot \log \left(\frac{NSD_{Sys}}{NSD_{Ref}} \right) = 10 \cdot \log \left(\frac{5.3 \cdot 10^{-21}}{1} \right) = -202.8 \text{ dBW Hz}^{-1}$$

Noise spectral density from the antenna: For the quiet Sun to be detected, the antenna output noise spectral density NSD_{Ant} must be higher than the system noise floor. This can be expressed in terms of a margin M in dB such that

$$NSD_{Ant} (\text{dBW / Hz}) \geq NSD_{Sys} + M \text{ dBW Hz}^{-1} \quad (4)$$

Example 1: Find the noise spectral density at the antenna for emissions that are $M = 5$ dB above the system noise floor. Assume the LNA noise figure is 1.1 dB.

Solution: Using eq. (4), the input to the low noise amplifier from the antenna (assuming zero loss in the connection) needs to be

$$NSD_{Ant} \text{ (dBW / Hz)} \geq -202.8 + 5 = -197.8 \text{ dBW Hz}^{-1}$$

As a linear ratio, the required input noise spectral density from the quiet Sun for this example is

$$NSD_{Ant} = 10^{\left(\frac{NSD_{Ant} \text{ (dBW/Hz)}}{10}\right)} \geq 10^{\left(\frac{-197.8}{10}\right)} = 1.7 \cdot 10^{-20} \text{ W Hz}^{-1}$$

The required noise spectral density at the antenna is related to the quiet Sun spectral flux density S_{Quiet} and antenna effective area A_{Eff} by

$$NSD_{Ant} = \frac{S_{Quiet} \cdot A_{Eff}}{2} \text{ W Hz}^{-1} \quad (5)$$

where S_{Quiet} is the spectral flux density of the quiet Sun at the frequency of interest in $\text{W m}^{-2} \text{ Hz}^{-1}$ and A_{Eff} is the antenna effective area in m^2 . The divisor 2 takes into account that a linear polarized antenna captures only one-half the total flux from a randomly polarized radio source.

Solving eq. (5) for the antenna effective area gives

$$A_{Eff} = \frac{2 \cdot NSD_{Ant}}{S_{Quiet}} \quad (6)$$

Antenna gain: The antenna gain G with respect to an isotropic antenna is related to the antenna effective area and wavelength by

$$G = A_{Eff} \cdot \frac{4 \cdot \pi}{\lambda^2} \quad (7)$$

where the antenna gain is a linear ratio. The wavelength is related to the frequency by

$$\lambda = \frac{c}{f} \quad (8)$$

where c is the speed of light ($3 \cdot 10^8 \text{ m s}^{-1}$) and f is the frequency in Hz. The antenna effective area is related to its physical aperture area A_{Phys} by

$$A_{Eff} = \eta \cdot A_{Phys} \quad (9)$$

where η is the aperture efficiency (for ordinary parabolic dish antennas η is typically 0.5 to 0.55).

Substituting eq. (6) in (7) and simplifying gives the required antenna gain in terms of the system noise spectral density, quiet Sun spectral flux density and wavelength, as in

$$G = \frac{8 \cdot \pi \cdot NSD_{Ant}}{S_{Quiet} \cdot \lambda^2} \quad (10)$$

Example 2: Find the antenna gain required to detect the quiet Sun at 200 MHz with a 5 dB margin.

Solution: From eq. (8), the wavelength at 200 MHz is

$$\lambda = \frac{c}{f} = \frac{3 \cdot 10^8}{200 \cdot 10^6} = 1.5 \text{ m}$$

From table 1, the spectral flux density of the quiet Sun S_{Quiet} at 200 MHz is 8.1 sfu or $8.1 \cdot 10^{-22} \text{ W m}^{-2} \text{ Hz}^{-1}$. The required antenna noise spectral density for margin $M = 5 \text{ dB}$ from Example 1 is $1.7 \cdot 10^{-20} \text{ W Hz}^{-1}$. Substituting values for the wavelength, quiet Sun spectral flux density and required antenna noise spectral density into equation (10) gives

$$G = \frac{8 \cdot \pi \cdot NSD_{Ant}}{S_{Quiet} \cdot \lambda^2} = \frac{8 \cdot \pi \cdot 1.7 \cdot 10^{-20}}{8.1 \cdot 10^{-22} \cdot 1.5^2} = 234.4$$

The gain in dB with respect to an isotropic antenna is

$$G(\text{dB}) = 10 \cdot \log(G) = 10 \cdot \log(234.4) = 23.7 \text{ dBi}$$

A higher or lower margin requires a higher or lower antenna gain; however, when expressed in dB the two are not exactly proportional. In the example above, increasing M by 1 dB from 5 to 6 dB increases the required noise spectral density from $1.7 \cdot 10^{-20}$ to $2.1 \cdot 10^{-20} \text{ W Hz}^{-1}$. The required antenna gain as a linear ratio is increased from 234.4 to 288.1, corresponding to 24.6 dBi, an increase of 0.9 dB. Similar calculations for a 1 dB decrease in the margin show that the required antenna gain is decreased by 1.1 dB from 23.7 to 22.6 dBi.

Antenna beamwidth: The high gain antennas required to receive the quiet Sun have narrow beamwidths compared to ordinary dipole and LPDA antennas and will require tracking the Sun during the eclipse. The half-power beamwidths (HPBW) can be determined from the antenna directivity. Directivity is a calculated parameter similar to gain whereas gain is a measured parameter that includes antenna losses and is always smaller than directivity. The ratio of gain to directivity is the *antenna efficiency factor* k_{Ant} .

For an antenna with minor lobes (side lobes and back lobes found on all practical antennas) and non-ideal radiation patterns, the directivity D , from [Kraus], is

$$D \approx \frac{41000 \cdot \varepsilon_M}{k_p \cdot \theta_{HP}^\circ \cdot \phi_{HP}^\circ} \quad (11)$$

where

ε_M beam efficiency, 0.6 to 0.9 for large antennas

k_p pattern factor, 1.0 for uniform field distribution, between 0 and 1 otherwise

θ_{HP}° half-power beamwidth in θ plane (for example, E-plane) ($^\circ$)

ϕ_{HP}° half-power beamwidth in ϕ plane (for example, H-plane) ($^\circ$)

Assuming the antenna efficiency factor k_{Ant} is close to 1, the pattern is uniform and symmetrical in any plane ($\theta_{HP}^\circ = \phi_{HP}^\circ$) and the beam efficiency is in the mid-range, eq. (11) reduces to

$$G \approx \frac{30750}{(\theta_{HP}^\circ)^2} \quad (12)$$

Solving for θ_{HP}° gives a reasonable estimate of the HPBW, or

$$\theta_{HP}^\circ \approx \left(\frac{30750}{G} \right)^{\frac{1}{2}} \quad (13)$$

Example 3: Estimate the half-power beamwidth for the antenna in Example 2.

Solution: The gain previously determined is 234.4 or 23.7 dB. The beamwidth calculation requires the gain as a linear ratio. From eq. (13)

$$\theta_{HP}^\circ \approx \left(\frac{30750}{G} \right)^{\frac{1}{2}} = \left(\frac{30750}{234.4} \right)^{\frac{1}{2}} = 11.5^\circ$$

Calculations for gain and beamwidth can be made for various spot frequencies previously given for the quiet Sun and summarized (table 2).

Table 2 ~ Antenna gains required for detecting the quiet Sun with 5 dB margin and corresponding half-power beamwidths. Quiet Sun data is from table 1. LNA noise figure = 1.1 dB, zero loss between the antenna and LNA.

Frequency (MHz)	Wavelength (m)	S _{Quiet} (sfu)	S _{Quiet} (W m ⁻² Hz ⁻¹)	Gain (dBi)	Gain (linear)	HPBW (°)
50	6	0.54	0.54 · 10 ⁻²²	23.4	219.8	11.8
100	3	2.4	2.4 · 10 ⁻²²	23.0	197.8	12.5
150	2	5.1	5.1 · 10 ⁻²²	23.2	209.4	12.1
200	1.5	8.1	8.1 · 10 ⁻²²	23.7	234.4	11.5
300	1	14.9	14.9 · 10 ⁻²²	24.6	286.8	10.4
400	0.75	21.7	21.7 · 10 ⁻²²	25.4	350.0	9.4
600	0.5	32.1	32.1 · 10 ⁻²²	27.3	532.4	7.6
1000	0.3	41.3	41.3 · 10 ⁻²²	30.6	1149.5	5.2
10000	0.03	275	275 · 10 ⁻²²	42.4	17263	1.3

The required gains can be achieved in a number of ways. For example, a stacked array of multi-element Yagi antennas or a parabolic dish antenna may be used (figure 10). Yagi antenna bandwidth is only about 5% of the center frequency and stacking in an array increases the gain but usually reduces the bandwidth. An alternative with a bandwidth in the range of 50% of the center frequency is a stacked array of helical antennas (more specifically, monofilar, axial mode helical antennas). Detailed information on helical antennas can be found at [Kraus]. Both Yagi and helical antennas can be used as feeds on parabolic dish reflector antennas.



Figure 10 ~ 5m parabolic dish at radio astronomy facility of ETH Zurich in Bleien. Box behind feed contains band pass filters and a low noise amplifier. While tracking the Sun, the entire antenna rotates in azimuth and in elevation controlled by a standard Windows computer. The estimated gain of is 45 dBi in L-band. Tower carrying the dish is a spotlight structure from WW-II. The shade of the focal plane unit in the dish center proves that the dish is tracking the sun. This dish antenna was used to produce the light-curve plot, shown in figure 15. Image courtesy of C. Monstein.

The physical area of a parabolic dish antenna is

$$A_{phys} = \frac{\pi \cdot d^2}{4} \tag{14}$$

where d is the dish diameter. Using eq. (9) and assuming the aperture efficiency $\eta = 0.55$, the effective area of a parabolic dish antenna is

$$A_{\text{eff}} = \eta \cdot A_{\text{phys}} = 0.55 \cdot \frac{\pi \cdot d^2}{4} \quad (15)$$

Substituting eq. (15) in eq. (7) gives the gain in terms of the dish diameter and wavelength, or

$$G = \eta \cdot \frac{\pi \cdot d^2}{4} \cdot \frac{4 \cdot \pi}{\lambda^2} = \eta \cdot \frac{\pi^2 \cdot d^2}{\lambda^2} \quad (16)$$

Solving for the diameter d gives

$$d = \frac{\lambda}{\pi} \left(\frac{G}{\eta} \right)^{\frac{1}{2}} \quad (17)$$

Assuming $\eta = 0.55$,

$$d = 1.35 \cdot \frac{\lambda}{\pi} G^{\frac{1}{2}} = 0.43 \cdot \lambda \cdot G^{\frac{1}{2}} \quad (18)$$

Example 4: Determine the diameter of a parabolic dish antenna that provides the gain found in Example 2.

Solution: The required gain was found to be 23.7 dBi or linear ratio 234.4 for a wavelength of 1.5 m. Substituting these values in eq. (18) gives

$$d = 1.35 \cdot \frac{1.5}{\pi} 234.4^{\frac{1}{2}} = 9.9 \text{ m}$$

It is noted that this size of parabolic dish antenna usually is found only in professional observatories, although it is known that at least one amateur radio observatory has an antenna at least as large [{Astropeiler}](#).

Combining eq. (13) and (16), the beamwidth of a parabolic dish antenna in terms of its diameter and wavelength is approximately

$$\theta_{\text{HP}}^{\circ} \approx \frac{\lambda}{d} \left(\frac{30750}{\eta \cdot \pi^2} \right)^{\frac{1}{2}} \quad (19)$$

Assuming $\eta = 0.55$,

$$\theta_{\text{HP}}^{\circ} \approx 75.3 \frac{\lambda}{d} \quad (20)$$

The above calculations concerning parabolic dish antennas assume that all incoming flux is reflected toward and captured by their associated feed antennas. Antenna design is beyond the scope of this paper; readers are referred to [Kraus] and other antenna engineering books and online resources.

8. Ku Band Down-Converter for X-Band Observations

In this section we discuss using a low-cost Ku-band dish antenna and associated low noise block converter (LNB) designed for satellite television reception with Callisto to observe the solar eclipse. These can provide an inexpensive alternative to constructing an antenna array or large parabolic reflector antenna. The actual observation frequency will be closer to about 10.6 GHz (X-band), which will be down-converted by the LNB to the Callisto native frequency range. The advantage of using Callisto with this setup is its reliability, consistency and data collection and processing capability. The technical requirements are not critical but a bias-tee (also called *power inserter* or *power injector* in the satellite television industry) will be needed to power the LNB (figure 11).

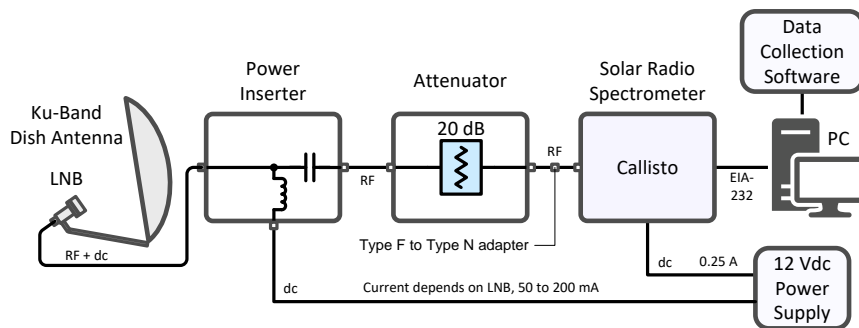


Figure 11 ~ Block diagram for observing at X-band using a Ku-band dish antenna, LNB and Callisto. An attenuator is optional to minimize receiver input overload. All coaxial cabling from the LNB to Callisto uses RG-6 (or equivalent) with type F connectors. A type F to type N adapter connects to the Callisto.

Example 5: Determine the diameter of a parabolic dish antenna that provides a 5 dB margin for detecting quiet Sun radio emissions at 10 GHz.

Solution: Table 2 shows that the necessary gain at 10 GHz is 42.4 dBi or 17 263 and the wavelength is 0.03 m. Substituting these values in eq. (18) gives

$$d = 1.35 \cdot \frac{0.03}{\pi} 17263^{\frac{1}{2}} = 1.7 \text{ m}$$

It is noted that a common commercial dish size is 1.65 m. A larger dish will provide a more pronounced Y-factor (ratio of Sun noise temperature-to-Sky noise temperature) and improve the detection margin as the Sun's flux is reduced during the eclipse.

Example 6: Determine the aperture efficiency, antenna noise temperature and half-power beamwidth at 10 GHz for an inexpensive 18 in diameter offset feed dish antenna (figure 12). The manufacturer's claim is its effective aperture is 18.1 in (46 cm).



Figure 12 ~ Inexpensive 46 cm diameter offset feed dish antenna and LNB originally designed for satellite television

Solution: The actual measured dimensions of this antenna from edge-to-edge are 18.25 W x 20.0 H in (46.4 W x 50.8 H cm). Assuming the antenna shape is an ellipse, its physical area

is $\pi \cdot \frac{W \cdot H}{4} = 287 \text{ in}^2$ (0.185 m²). Also, assuming the

manufacturer's claim applies to a circular aperture, the

aperture area is $\pi \cdot \frac{d^2}{4} = 257 \text{ in}^2$ (0.166 m²) and the aperture

efficiency $\eta = \frac{A_{\text{Eff}}}{A_{\text{Phys}}} = \frac{257}{287} = 0.9$ (this seems to be overstated by a factor of 2).

From table 1 (or table 2) the spectral flux density from the quiet Sun at 10 GHz is 275 sfu or, equivalently, $275 \cdot 10^{-22} \text{ W m}^{-2} \text{ Hz}^{-1}$. Based on the effective area previously calculated, the noise spectral density at the antenna from eq. (5) is

$$NSD_{\text{Ant}} = \frac{S_{\text{Quiet}} \cdot A_{\text{Eff}}}{2} = \frac{275 \cdot 10^{-22} \cdot 0.166}{2} = 2.28 \cdot 10^{-21} \text{ W Hz}^{-1}$$

The antenna noise temperature T_{Ant} is related to the antenna noise spectral density by the Boltzmann constant k , or

$$NSD_{\text{Ant}} = k \cdot T_{\text{Ant}}$$

Therefore, the antenna noise temperature is

$$T_{\text{Ant}} = \frac{NSD_{\text{Ant}}}{k} = \frac{2.28 \cdot 10^{-21}}{1.38 \cdot 10^{-23}} = 165 \text{ K}$$

Because this calculation is traceable to the manufacturer's claim of the antenna's effective aperture, the antenna temperature may be overstated. Assuming the aperture efficiency is as the manufacturer claims ($\eta = 0.9$), from eq. (19) the HPBW of the antenna is approximately

$$\theta_{\text{HP}}^{\circ} \approx \frac{\lambda}{d} \left(\frac{30750}{\eta \cdot \pi^2} \right)^{\frac{1}{2}} = \frac{0.03}{0.46} \left(\frac{30750}{0.9 \cdot \pi^2} \right)^{\frac{1}{2}} = 3.8^{\circ}$$

Based on the specification of a standard commercial wideband LNB with 10.41 GHz local oscillator frequency, the LNB intermediate frequency (IF) ranges from (10.7 – 10.41 GHz =) 290 MHz to (11.28 GHz – 10.41 GHz =) 870 MHz. However, there is hardly any bandpass filtering in either the RF or IF paths of the LNB, so observations are possible below the low band frequency (figure 13). This unadvertised but free feature allows us to use Callisto as a down-converter spectrometer to observe the X-band (X-band is 7 to 11.2 GHz for NATO or 8 to 12.0 GHz according to IEEE). The usable observation bandwidth is limited by Callisto’s maximum frequency to about 580 MHz. Taking into account the LNB’s high sensitivity and IF output within Callisto’s frequency range, we can define the received frequency range as $F_{min} = 10.6$ GHz to $F_{max} = 10.72$ GHz.

The corresponding observation parameters are:

- ⊗ RF input frequency range: 10 600 MHz to 10 720 MHz
- ⊗ IF output frequency range: 290 to 870 MHz
- ⊗ Callisto channelization: 200 channels
- ⊗ Callisto frequency resolution: 2.9 MHz (580 MHz/200 channels)
- ⊗ Callisto detection bandwidth: 300 kHz
- ⊗ Callisto time resolution: 0.25 s
- ⊗ Callisto integration time: 1 ms
- ⊗ Duration of observation: 3 h

The Callisto frequency file can be setup with light curve integration assigned on channels 10 to 199 (channels 1 to 9 are not used to avoid the redundant channels always placed at the beginning of the frequency file; refer to the Callisto Software Setup Guide {[CallistoSSG](#) for more information}. For this situation, the usable observational bandwidth is 190 used channels x 2.9 MHz frequency resolution = 163.9 MHz, and the radiometric bandwidth is 149 used channels x 300 kHz detection bandwidth = 44.7 MHz. For a quiet Sun flux of about 275 sfu we may expect an antenna temperature on the order of 40 K.

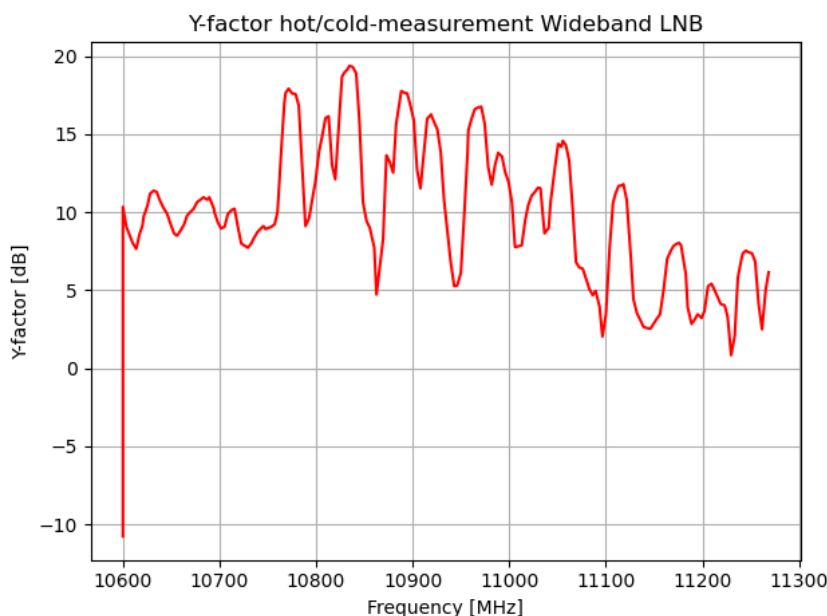


Figure 13 ~ Plot of the band pass characteristic and Y-factor of a wideband Ku-band LNB. Interestingly the LNB is most sensitive around 10.65 GHz below the regular band. Observations were performed with a hot/cold measurement. Hot while pointing to the sun and cold while pointing to the sky. Above 10.75 GHz we can see many satellite downlink transponders signals (TV), therefore we can only use frequencies below 10.75 GHz for radio astronomy.

There are three advantages to using an inexpensive LNB. First, is its very low cost (< 50 USD). Second, the noise figure of modern LNBs is less than 0.5 dB. The corresponding noise temperature is about 35 K, which is lower than the expected antenna noise temperature from the quiet Sun. Third, there is very little radio frequency interference (RFI) in the X-band and the observed spectrum is extremely clean, which allows undisturbed solar radio observations. From experience we do not expect high dynamic solar radio spectra in this frequency range, although some synchrotron radiation is remotely possible.

Unfortunately there are negative aspects in such an observation concept. The satellite dish, providing a small beam angle on the order of a few degrees as determined from eq. (19) requires constant tracking of the Sun during the whole observation from sunrise to sunset. Without tracking, we will observe strong variations in the signal due to the convolution of the antenna beam pattern and the moving solar disc, and these are indistinguishable from the signal drop due to the eclipse itself. A way to avoid this is to use an existing optical telescope with a computer that allows tracking the Sun, and to replace the optics with a small satellite dish and LNB combination.

Most modern inexpensive Ku-band satellite dishes are offset feed dishes, which make the alignment difficult. Offset angles are typically 17 to 24° (figure 14). A dish with a central axis (prime focus) feed is of great advantage because alignment is much simpler. In any case, an alignment is required a few days before the eclipse to ensure that the dish is correctly pointing to the Sun. The easiest way to adjust the offset dish is to move the antenna so that the LNB horn (the part closest to the antenna) casts a shadow at the edge of the antenna next to the LNB mounting arm. Another method involves using double-sided tape to attach a small mirror to the center of the dish and adjusting the antenna until the Sun's reflection shines on the LNB horn (remove the mirror when done). The central axis dish is adjusted so the LNB casts a shadow at the center of the dish. Of course, the shadow method works only when the Sun is visible. Once adjusted just start the solar tracker for the coming eclipse day.

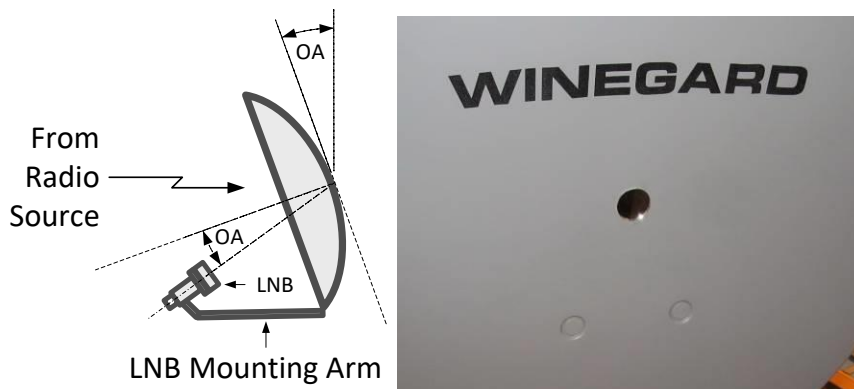


Figure 14 ~ Offset feed dish antenna. Left: Typical offset angles OA are 17 to 24°. Right: One method to align the antenna on a sunny day is to tape a small mirror to the dish center and then adjust the antenna so the Sun's reflection shines on the center of the LNB. A 25 mm diameter mirror from a local craft store is shown in this image attached to the center of a Winegard 46 cm dish.

Another difficulty is that inexpensive LNBs are sensitive to temperature and considerable drift can be expected if exposed to direct sunlight during observations. This can be at least partially mitigated by using a Sun shade on the LNB that is transparent to microwaves but this considerably complicates setting up. The least temperature disturbance can be expected on a cloudy day in which there is no direct sunlight on the LNB but this prevents alignment using the shadow method.

In spite of the above difficulties, a system composed of a satellite dish, LNB, Bias-T and Callisto is a quite convenient and attractive spectrometer to observe the quiet Sun and to estimate solar radio flux at microwave

frequencies. It also is an easy way to observe the signal drop due to the eclipse. Afterwards, the data can be calibrated in solar flux units (sfu) (figure 15) by taking into account the solar radio flux published by NOAA, SWS [{Learnmonth}](#) and others for the period. Observers considering this setup should look at the documents available for the Very Small Radio Telescope (VSRT) at [{Haystack}](#).

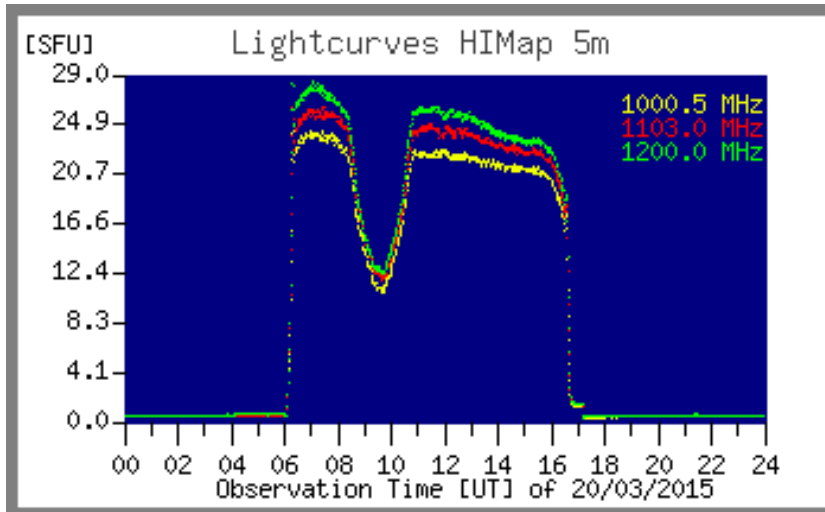


Figure 15 ~ Plot of an European eclipse on 20 March 2015, observed with a 5 m dish, tracking the Sun from Sunrise at around 06 UT until Sunset at 16:45 UT. The eclipse started around 08:30 with maximum obscuration at 09:30 and finished at 11:00. Calibration was performed based on reference values of the quiet Sun. Backend instrument was a Callisto frequency agile spectrometer, connected to a heterodyne converter which shifts 1-2 GHz down to 0-1GHz. For more details, see [Monstein]. We may expect a similar plot in X- or Ku-band performed with a ~60 cm satellite dish.

9. Scintillation Observations

This section briefly describes observations of satellite signals in the 250 MHz range to determine eclipse effects, if any, on radio wave scintillation. Additional information on scintillation can be found at [{SWS}](#).

Scintillation Effects: Scintillation is a random fluctuation in the intensity of celestial radio waves and satellite downlink signals on the time scale of a few seconds produced by ionospheric irregularities. Scintillation causes the familiar twinkling of visible light from stars and can be particularly detrimental at radio frequencies below a few gigahertz. A large amount of work has been done studying scintillation effects at L-band (1 to 2 GHz) on the accuracy of global navigation satellite systems (GNSS) such as the Global Positioning System (GPS). Signals from other satellites and spacecraft are affected as well. In the field of radio astronomy, scintillation can introduce undesired variations in the measurements of celestial radio objects.

Scintillation effects are broadly classified as refraction and diffraction. Both originate in the group delay and phase advance that a radio wave experiences as it interacts with free electrons along its transmission path through the ionosphere. The following discussion will focus on satellite signals because they are easily received by Callisto with an ordinary antenna and preamplifier.

The number of free electrons is usually expressed as *total electron content* (TEC), which is the number of free electrons in a rectangular solid with a one square meter cross-sectional area extending from the receiver to the satellite. Given by physics, the

The Total Electron Content (TEC) is the total number of electrons present along a path between a radio transmitter and receiver. Radio waves are affected by the presence of electrons. The more electrons in the path of the radio wave, the more the radio signal will be affected. TEC is a good parameter to monitor for possible space weather effects.

product of the group velocity and phase velocity of the satellite signals is equal to the speed of light squared. If the TEC increases, the signal's group velocity decreases and its phase velocity increases to keep their product a constant. A slower group velocity produces ranging errors in GPS systems while a faster phase velocity causes unexpected phase shifts. If the phase shifts are rapid enough, they can overwhelm the tracking loops in GPS receivers' phase-lock loops. Variations in group delay and phase advance caused by large-scale variations in electron density are defined as signal refraction.

Scintillation through signal diffraction is more complicated. When ionospheric irregularities form at scale lengths of a few hundred meters, they begin to scatter satellite signals causing the radio wave to follow multiple paths to the receiver. The signals on each path will add or subtract in phase, causing fluctuations in the signal amplitude and phase. The same process occurs with light and can be seen in the fuzzy image passing through jet exhaust from an airliner. Diffractive scintillation can seriously challenge GPS receivers, causing signal power fades exceeding several dB and fast phase variations.

The upcoming total solar eclipse will not affect all regions of the earth equally, and the physics behind the space weather in different regions can be dramatically different. The change in density and thickness of the ionosphere during the eclipse could potentially change radio waves traversing the ionosphere along the path of the shadow to a receiver.

Scintillation is quantified by an S4 index defined by

$$S4 = \sqrt{\frac{\langle I^2 \rangle - \langle I \rangle^2}{\langle I \rangle^2}} \quad (21)$$

where I is the signal intensity and the brackets ' $\langle \rangle$ ' denote time averages.

The S4-index can vary from 0 to 1.0 and is typically estimated over an interval of 60 seconds. The index can be considered weak or strong, roughly corresponding to the amount of scattering in the ionosphere. Strong scintillation corresponds to $S4 > 0.6$ and weak scintillation is $S4 < 0.6$. It has been determined that $S4 < 0.3$ is unlikely to have a significant effect on GPS signals.

A Python script [{S4FITS}](#) has been made available to perform the S4-index calculations from the FITS files produced by the Callisto spectrometer. For a moving satellite such as GPS or Iridium the calculations are applied over a time period of typically 5 to 10 s while for geostationary satellites the period can extend up to 60 seconds. The latter corresponds to a few hundred samples (480 samples at 100 channels/sweep or 240 samples at 200 channels/sweep; note: 1 sweep requires 0.25 s) per S4-index based on a Callisto system. We will concentrate on geostationary satellites because no tracking mechanism is needed and the frequencies fall within the Callisto frequency range. The S4-index will be plotted with respect to the elapsed time of observation.

Observing scintillation: Observing signals in the upper-VHF band from geostationary satellites provides a significant advantage over celestial emissions because the spectral flux density of the satellite signals is much higher at about -190 dBW $m^2 Hz^{-1}$. The high received power levels allow the use of relatively small and cheap antennas fixed in sky-position (azimuth and elevation) while pointing to the geostationary path of the desired

satellites. In addition to a ‘normal’ sensitivity receiver like Callisto, a standard low noise amplifier (LNA) is recommended between the antenna and Callisto to provide an adequate system noise figure. Of course, other receivers can be used for this experiment in a single frequency or single channel mode, but the Python script provided is based on reading FITS files.



Figure 16 ~ Log periodic dipole array antenna (LPDA) mounted on a mast with a rotator and low noise amplifier. The 21-element Creative Design CLP5130-1N antenna frequency range is 50 to 1300 MHz and its free space gain is 6 to 8 dB. This antenna installation has a fixed elevation but can be turned to any hour angle with the rotator. The low noise amplifier has a noise figure of about 1.0 dB and a gain of about 20 dB. Setup at University of Glasgow, UK. Image ©2012 C. Monstein.

For receiving satellite signals we can use a simple Yagi antenna or a logarithmic periodic dipole array, LPDA (figure 16) fixed in azimuth and elevation and pointing to the geostationary satellite path over Earth’s equator. An example is provided below. The azimuth and elevation will need to be separately determined for each location along the path of the eclipse. An online tool to find these angles can be found at {[GeoSat1](#)} and {[GeoSat2](#)}. Also, we provide a Python script {[GeoAzEl](#)} for calculating the necessary parameters for military satellites over North America. Each observer should try to choose a satellite near their local meridian.

It should be possible to observe downlinks in the frequency range 240 MHz to 270 MHz from UFO-*, Skynet, Fltsatcom, Sicral, ComsatBW and Milstar satellites. For example, see [UHFSatNA](#) for a list of satellites and their approximate longitudes that may be observable over North America. For a more comprehensive list of satellites worldwide see [UHFSat](#).

Example 7: Suppose we would like to detect the satellite signals with a 5 dB signal-to-noise ratio (equivalent to a 5 dB margin used in the example quiet Sun calculations shown previously). The noise figure of our low noise amplifier is 1.1 dB, as before. Find the required antenna gain.

Solution: The system noise spectral density was previously found in section 7 to be $-202.8 \text{ dBW Hz}^{-1}$ and to provide a 5 dB margin, the required antenna spectral density was $-197.8 \text{ dBW Hz}^{-1}$. In linear terms

$$NSD_{Ant} = 10^{\left(\frac{NSD_{Ant}(dB)}{10}\right)} \geq 10^{\left(\frac{-197.8}{10}\right)} = 1.7 \cdot 10^{-20} \text{ W Hz}^{-1}$$

The estimated received spectral flux density from the satellites is $S_{Sat} = -190 \text{ dBW m}^2 \text{ Hz}^{-1}$ or in linear terms

$$S_{Sat} = 10^{\frac{S_{Sat}(dB)}{10}} = 10^{\frac{-190}{10}} = 1.0 \cdot 10^{-19} \text{ W m}^2 \text{ Hz}^{-1}$$

From equation (6), the required antenna effective area is

$$A_{Eff} = \frac{2 \cdot NSD_{Ant}}{S_{Sat}} = \frac{2 \cdot 1.7 \cdot 10^{-20}}{1.0 \cdot 10^{-19}} = 0.340 \text{ m}^2$$

For a mid-range frequency of 255 MHz, the wavelength from equation (8) is

$$\lambda = \frac{c}{f} = \frac{3 \cdot 10^8}{255 \cdot 10^6} = 1.18 \text{ m}$$

From equation (7), the antenna gain in terms of its effective area and wavelength is

$$G = A_{Eff} \cdot \frac{4 \cdot \pi}{\lambda^2} = 0.340 \cdot \frac{4 \cdot \pi}{(1.18)^2} = 3.09$$

As a logarithmic ratio in dB with respect to an isotropic antenna, the required gain is

$$G(dB) = 10 \cdot \log(G) = 10 \cdot \log(3.09) = 4.9 \text{ dBi}$$

Thus, with the assumptions given above, we find the antenna requirements are quite modest and can be easily fulfilled with almost any Yagi or log periodic antenna.

The scanning strategy for these satellites can use a Callisto frequency configuration file with 100 channels. In this case, each channel would cover (270 - 240) MHz/100 channels = 0.3 MHz, which equals the radiometric bandwidth of the Callisto radio spectrometer. Such a strategy will ensure we do not miss any transmission channels from the observed satellites.

For comparison purposes, Callisto should be setup to observe before and after the eclipse using a similar routine as described for observing the solar emissions in section 4. After the FITS files are saved and post-processed by the above-mentioned {S4FITS} Python script the S4 scintillation index is plotted versus time for any channel in the above frequency range. While we expect a change in the S4-index during the eclipse, it is yet to be proven to what extent the change will be.

10. Conclusions

The total solar eclipse on 8 April 2024 provides a great opportunity for solar radio observations in the VHF and UHF bands using the Callisto instrument. As the Moon's shadow crosses the United States it will block radio emissions from the quiet Sun. Callisto stations will need to add a low noise amplifier, if not already equipped, and upgrade their antennas to detect the quiet Sun. Two inexpensive alternative observations also are

discussed, one to use a dish antenna and LNB designed for satellite television reception to observe the quiet Sun and another to observe geostationary satellite transmissions in the upper-VHF band and determine changes, if any, in the S4 scintillation index during the eclipse. To be most successful observers should start planning and rehearsing now for the event.

11. Weblinks and References

- {Astropeiler} <https://astropeiler.de/>
 - {Callisto} <http://www.reeve.com/Solar/e-CALLISTO/e-callisto.htm>
 - {CallistoSSG} <http://www.reeve.com/Documents/CALLISTO/CALLISTOSoftwareSetup.pdf>
 - {eCallisto} <https://www.e-callisto.org/>
 - {GE-Eclipse} http://xjubier.free.fr/en/site_pages/solar_eclipses/TSE_2017_GoogleMapFull.html
 - {GeoAzEl} <https://e-callisto.org/Software/GeoAzEl.py>
 - {GeoSat1} <http://www.csgnetwork.com/geosatposcalc.html>
 - {GeoSat2} <http://www.dishpointer.com/>
 - {Haystack} <http://www.haystack.edu/edu/pcr/vsrt-ret/index.html>
 - {Learmonth} <http://www.sws.bom.gov.au/Solar/3/4>
 - {MICA} <http://aa.usno.navy.mil/software/mica/micainfo.php>
 - {NASA} <http://eclipse.gsfc.nasa.gov/SEgoogle/SEgoogle2001/SE2017Aug21Tgoogle.html>
 - {NOAA} <https://www.esrl.noaa.gov/gmd/grad/solcalc/>
 - {Path} <https://eclipse.gsfc.nasa.gov/SEpath/SEpath2001/SE2017Aug21Tpath.html>
 - {Solar} <http://www.timeanddate.com/eclipse/list.html%3Fstarty%3D1950>
 - {S4FITS} <https://e-callisto.org/Software/S4FITS.zip>
 - {SWS} <http://www.sws.bom.gov.au/Satellite/6/3>
 - {UHFSat} <http://www.uhf-satcom.com/uhf/>
 - {UHFSatNA} <http://www.crypto.com/misc/uhf-sats/>
-
- [Benz] Benz, A., Chapt. 4.1.1.6 Radio Emission of the Quiet Sun, Solar System, Springer, DOI: 10.1007/978-3-540-88055-4_5, 2009
 - [Kraus] Kraus, J., Antennas, 2nd Ed., McGraw-Hill Inc., 1988
 - [Kundu] Kundu, M., Solar Radio Astronomy, John Wiley & Sons, 1965
 - [Monstein] Monstein, C., European Solar Eclipse Observed by Radio Waves, *Radio Astronomy*, March- April 2015, pages 21-27
 - [ReeveLNA] Reeve, W., Packaging a Low Noise RF Amplifier Module, *Radio Astronomy*, September-October 2015
 - [Smerd] Smerd, S., Radio-Frequency Radiations from the Quiet Sun, Australian Journal of Scientific Research A, vol. 3, p.34, 1950 (available at: <http://adsabs.harvard.edu/full/1950AuSRA...3...34S>)